

Differential roles of serotonin receptor subtypes in regulation of neurotrophin receptor expression and intestinal hypernociception

Meng-Ping She¹, Yu-Ting Hsieh¹, Li-Yu Lin¹, Chia-Hung Tu²,
Ming-Shiang Wu², Ling-Wei Hsin^{3,4} and Linda Chia-Hui Yu¹

¹Graduate Institute of Physiology, National Taiwan University College of Medicine, ²Department of Internal Medicine, National Taiwan University Hospital and College of Medicine, ³School of Pharmacy, National Taiwan University and ⁴Center for Innovative Therapeutics Discovery, National Taiwan University, Taipei, Taiwan ROC

Summary. Objectives. Aberrant serotonin (5-hydroxytryptamine, 5-HT) metabolism and neurite outgrowth were associated with abdominal pain in irritable bowel syndrome (IBS). We previously demonstrated that 5-HT receptor subtype 7 (5-HT₇) was involved in visceral hypersensitivity of IBS-like mouse models. The aim was to compare the analgesic effects of a novel 5-HT₇ antagonist to reference standards in mouse models and investigate the mechanisms of 5-HT₇-dependent neuroplasticity.

Methods. Two mouse models, including *Giardia* post-infection combined with water avoidance stress (GW) and post-resolution of trinitrobenzene sulfonic acid-induced colitis (PT) were used. Mice were orally administered CYY1005 (CYY, a novel 5-HT₇ antagonist), alosetron (ALN, a 5-HT₃ antagonist), and loperamide (LPM, an opioid receptor agonist) prior to measurement of visceromotor responses (VMR). Levels of nerve growth factor (NGF), brain-derived neurotrophic factor (BDNF), and neurotrophin receptors (NTRs) were assessed.

Results. Peroral CYY was more potent than ALN or LPM in reducing VMR values in GW and PT mice. Increased mucosal 5-HT₇-expressing nerve fibers were associated with elevated *Gap43* levels in the mouse colon. We observed higher colonic *Ntrk2* and *Ngfr* expression in GW mice, and increased *Bdnf* expression in PT mice compared with control mice. Human SH-SY5Y cells stimulated with mouse colonic supernatant or exogenous serotonin exhibited longer nerve fibers, which CYY dose-dependently inhibited. Serotonin increased *Ntrk1* and *Ngfr* expression via 5-HT₇ but not

5-HT₃ or 5-HT₄, while *Ntrk2* upregulation was dependent on all three 5-HT receptor subtypes.

Conclusions. Stronger analgesic effects by peroral CYY were observed compared with reference standards in two IBS-like mouse models. The 5-HT₇-dependent NTR upregulation and neurite elongation may be involved in intestinal hypernociception.

Key words: Irritable bowel syndrome, Nerve hypersensitivity, Serotonin receptors, Neurotrophin receptors, Neurite outgrowth, Enteric nervous system

Introduction

Irritable bowel syndrome (IBS) is a functional bowel disorder in which relapsing abdominal pain or discomfort is associated with defecation or a change in bowel habit without detectable organic causes (Ford et al., 2020; BouSaba et al., 2022; Lambarth et al., 2022). A lower pain threshold to intestinal distension, which is referred to as visceral hypersensitivity, was reported in all IBS patients, irrespective of the defecation patterns (Ford et al., 2020; BouSaba et al., 2022; Lambarth et al., 2022). Altered intestinal serotonin/5-hydroxytryptamine (5-HT) metabolism, higher density of mucosal nerve fibers, and elevated levels of neurotrophins, such as nerve growth factor (NGF) and brain-derived neurotrophic factors (BDNF), are biomarkers correlative to abdominal pain scores in IBS patients (Atkinson et al.,

Abbreviations. IBS, Irritable bowel syndrome; 5-HT₇, 5-hydroxytryptamine receptor subtype 7; PGP9.5, protein gene product 9.5; NGF, nerve growth factor; BDNF, brain-derived nerve growth factor; Trk, Tropomyosin receptor kinase; p75^{NTR}, p75 neurotrophin receptor; TNBS, 2,4,6-trinitrobenzene sulfonic acid; PFA, paraformaldehyde; VMR, visceromotor response; CRD, colorectal distension; AUC, area under curve; LPM, loperamide; ALN, alosetron.

Corresponding Author: Linda Chia-Hui Yu, Professor, Graduate Institute of Physiology, National Taiwan University College of Medicine, Suite 1020, #1 Jen-Ai Rd. Sec. 1, Taipei 100, Taiwan ROC. e-mail: lchyu@ntu.edu.tw

www.hh.um.es. DOI: 10.14670/HH-18-687



2006; Dunlop et al., 2006; Yu et al., 2012; Dothel et al., 2015; Zhang et al., 2019).

Serotonin is initially identified as a brain neurotransmitter, which is now recognized as mainly (95%) produced by enteric nerves and enterochromaffin cells involved in bowel movement and pain sensation with neuroendocrine functions. Elevated 5-HT-dependent visceral hypersensitivity was reported in recipient animals intracolonicly infused with mucosal biopsy and fecal supernatant from IBS patients (Gao et al., 2022), and administration of exogenous 5-HT caused intestinal hyperalgesia in rat models (Cenac et al., 2010; Zhang et al., 2011). Expression of 5-HT receptor subtype 3 (5-HT₃), subtype 4 (5-HT₄), and subtype 7 (5-HT₇) have been reported in the intestinal tract; 5-HT₇ is the most recently discovered member of the receptor family (Kim and Khan, 2014; Lee et al., 2021). Our previous study demonstrated a reduction in intestinal pain by treatment with a novel 5-HT₇ antagonist, CYY1005 (CYY), in IBS-like mouse models (Chang et al., 2022). Other clinical medications for diarrhea-predominant IBS included alosetron (ALN, a 5-HT₃ antagonist) and loperamide (LPM, an opioid receptor agonist), while tegaserod (a 5-HT₄ agonist) was used for the management of constipation-predominant IBS. ALN and tegaserod improve symptoms but have severe side effects such as cerebrovascular and cardiovascular ischemia (Ford et al., 2009; Nee et al., 2015). Opiate agonists such as LPM are commonly used to correct bowel movements by reducing the peristaltic rate (Corsetti and Whorwell, 2017). In light of the fact that current treatments are ineffective for pain symptoms in IBS, the analgesic effects of peroral CYY are compared to ALN and LPM in this study.

Increased transcript levels of 5-HT₃ and 5-HT₇ were documented in colorectal tissues of diarrhea-predominant IBS patients (Ren et al., 2007; Zou et al., 2007; Yu et al., 2016), however, limited evidence of altered intestinal 5-HT₄ levels was found in IBS patients despite numerous studies using 5-HT₄ receptor agonists to target constipation symptoms (Fukudo et al., 2021). The expression of 5-HT₇ was observed on enteric neurons (Tonini et al., 2005; Dickson et al., 2010; Yaakob et al., 2015), lumbar dorsal root ganglia, and brain cortex and hippocampus regions (Meuser et al., 2002, Zou et al., 2007). In contrast, 5-HT₃ and 5-HT₄ receptor expression was identified in enteric nerves (Liu et al., 2005; Michel et al., 2005; Monro et al., 2005) and colonic epithelia (Ataee et al., 2010; Spohn et al., 2016). Recent reports demonstrated that 5-HT₃ was involved in serotonin-evoked ion secretion in mouse colonic organoids and epithelial 5-HT₄ activation increased fluid secretion in the proximal colon (Bhattarai et al., 2017, 2018). These findings suggest that interventions targeting 5-HT₃ and 5-HT₄ may partly be acting on epithelial ion fluxes while targeting 5-HT₇ mainly corrects neural sensation.

Neuroplasticity is crucial for neuronal repair and synapse formation, and modulates the magnitude of pain

sensation. Accumulating evidence indicates that nerve fiber outgrowth and neurotrophin levels are increased in the intestinal mucosa of IBS patients (Yu et al., 2012; Dothel et al., 2015; Zhang et al., 2019). Neurotrophins such as NGF and BDNF bind to neurotrophin receptors (NTRs) composed of subunits including high-affinity receptors, i.e., tropomyosin receptor kinase (Trk) A and B, in complex with the low-affinity p75^{NTR} (Khan and Smith, 2015). Previous work from our laboratory and others demonstrated that 5-HT₇ was involved in intestinal mucosal neurite outgrowth and forebrain synaptogenesis (Kobe et al., 2012; Speranza et al., 2017; Chang et al., 2022). A role of 5-HT₄ was also documented in dendrite sprouting for memory formation (Schill et al., 2020). To date, the differential roles of 5-HT receptor subtypes in regulating individual NTR subunit expression and neurite elongation remain unclear.

In the present study, two mouse models with visceral hypersensitivity were utilized to compare analgesic effects with peroral CYY against reference standards, such as ALN and LPM, clinically used for diarrhea-predominant IBS. Mucosal expression patterns of 5-HT receptor subtypes and the transcript levels of neurotrophins and NTRs were examined in mouse colonic tissues. The half-maximum inhibitory concentration (IC₅₀) of CYY on neurite outgrowth was determined in human neuronal cell cultures stimulated with bacteria-free colonic supernatants *in vitro*, and was compared to that of a putative 5-HT₇ receptor antagonist (SB-269970) known to be unstable via oral routes. Moreover, the roles of 5-HT receptor subtypes in the regulation of distinct NTR subunits were assessed.

Materials and methods

Animals

Specific pathogen-free C57BL/6 male mice (4-6 weeks of age) obtained from the National Taiwan University College of Medicine (NTUCM) animal facility were used for the study. Animals were raised in a temperature-controlled room (20±2°C) with 12/12-hour light/dark cycles and fed with regular chow and water *ad libitum*. All experimental procedures have been approved by the Institute of Animal Care and Use Committee (IACUC#20160288) of NTUCM.

Reagents

A novel 5-HT₇ antagonist, CYY1005 (PCT# WO2018157233 (A1)), was chemically synthesized by the laboratory of Dr. Hsin LW, School of Pharmacy, NTU. Reagents, such as SB-269970 hydrochloride (SB7, a selective 5-HT₇ antagonist), ALN (a selective 5-HT₃ antagonist), and LPM (an agonist to mu-, delta-, and kappa-opioid receptors), were purchased from Sigma-Aldrich (St. Louis, MO, USA). GR125487 (a selective 5-HT₄ antagonist) was purchased from Tocris

Bioscience (Minneapolis, MN, USA).

Mouse models of visceral hypersensitivity

Two mouse models of IBS-like visceral hypersensitivity were investigated, including one model with dual triggers of parasite postinfection combined with psychological stress, and the other one with post-resolution of 2,4,6-trinitrobenzene sulfonic acid (TNBS)-induced colitis (Feng et al., 2012; Chen et al., 2013; Lapointe et al., 2015; Halliez et al., 2016; Hsu et al., 2016). In the first model, mice were inoculated with *Giardia* (G) trophozoites on day 0 and subjected to water avoidance stress (WAS) during the post-clearance phase on days 42-51 (designated the GW model) (Chen et al., 2013; Hsu et al., 2016). Briefly, mice were orogavaged with 10⁷ *Giardia* trophozoites strain GS/M suspended in 0.2 ml of sterile saline. On the sixth week postinfection, when trophozoites cannot be detected in the intestine, mice were subjected to WAS for 1 hr/day for ten consecutive days, followed by measurement of intestinal pain on the last day of the stress session. The uninfected unstressed control (Ctrl) group was pair-fed with phosphate-buffered saline and left in cages unhandled.

In the second model, post-inflammatory pain was measured after the resolution of colitis induced by intracolonic injection of TNBS (Sigma) at 75 mg/kg body weight dissolved in 40% ethanol in a 0.2 ml volume of saline on day 0 (Feng et al., 2012; Lapointe et al., 2015; Halliez et al., 2016). The sham control (sham) group was intracolonicly injected with the same volume of saline on day 0. The time point of 24 days post-TNBS (designated the PT model) was chosen to represent persistent pain in the absence of inflammation, whereby our pilot study demonstrated the resolution of inflammatory parameters (i.e., myeloperoxidase activity and histopathological scores) seven days after TNBS injection (Chang et al., 2022). To test analgesic effects in the two models with visceral hypersensitivity, mice were perorally (p.o.) administered reagents at 5 mg/kg via a single dose in a saline vehicle 1.5 hours before intestinal pain measurement.

Assessment of pain sensation to colorectal distension

Abdominal pain was measured by visceromotor responses (VMRs) to colorectal distension (CRD) as previously described (Hong et al., 2011; Hsu et al., 2016; Chang et al., 2022). Briefly, electrodes made from Teflon-coated stainless-steel wire (A-M Systems, Carlsborg, WA) were implanted in the abdominal external oblique muscles of mice at least 14 days before VMR experiments, and the electrodes were exteriorized onto the back of the neck. The surgical procedure was granted by IACUC#20160288. Mice were habituated in the plexiglass cylinder for 30 minutes per day for three consecutive days before VMR experiments for acclimatization. For recording, electrodes were connected to an electromyogram acquisition system (AD

instruments, New South Wales, Australia). Mice were fasted overnight for the VMR tests, and the colon was distended by inflating a balloon catheter inserted intrarectally and subjected to four 10-second distensions (15, 40, and 65 mmHg) with 3-min rest intervals. The electromyographic (EMG) activity was amplified and digitized using a transducer (AD instruments) connected to a P511 AC amplifier (Grass Instruments, CA, USA) and Powerlab device with Chart 5 software (AD instruments). The EMG activity was rectified and the response was recorded as the increase in the area under the curve (AUC) of the EMG amplitude during CRD *versus* the baseline period.

Charcoal meal test

Mice were gavaged with 0.2 ml charcoal meal (3% arabic gum and 10% charcoal in PBS; Sigma) after the measurement of VMR. The intestinal tract was removed after thirty minutes and longitudinally dissected. Intestinal transit was defined as the position of the leading edge of the charcoal meal traveled as a percentage of the total length of the small and large intestine.

Histopathological examination

Intestinal tissues were fixed in 4% paraformaldehyde (PFA) and embedded in paraffin wax with proper orientation of the crypt to the villus axis before sectioning. Sections of 5- μ m thickness were deparaffinized with xylene and graded ethanol, stained with hematoxylin and eosin, and observed under a light microscope (Pai et al., 2021, 2023).

Immunofluorescent staining in intestinal tissues

Cryofixed sections post-fixed in acetone were incubated with 1% Triton X-100 for 10 minutes and then blocked with 1% bovine serum albumin (BSA) for two hours at room temperature. Tissue sections were incubated with primary antibodies, rabbit polyclonal anti-PGP9.5 (#39959) (1:250, GeneTex), anti-5-HT₇ (#ab61562) (1:200, Abcam, Burlingame, CA, USA), anti-5-HT₃ (#ab13897) (1:100, Abcam), anti-5-HT₄ (#ab60359) (1:200, Abcam), or isotype control IgG antibodies (#10500C, Invitrogen) overnight in a cold room (Matsumoto et al., 2012; Dothel et al., 2015). Negative controls by omitting primary antibodies were performed to confirm specific staining. The sections were washed with saline and incubated with a secondary goat anti-rabbit IgG conjugated to Alexa Fluor 488 (1:250, Invitrogen) for one hour at room temperature. Tissues were then incubated with a Hoechst dye (1 μ g/ml in PBS) (Sigma) for 30 minutes. The images were captured under a Zeiss microscope for quantification of fluorescence intensity by using imaging software (Axio Vision SE64, Zeiss, Oberkochen, Germany). Fluorescence intensity per area was quantified in five

images of the colonic mucosa per mouse and in five mice per group. A total of 25 images from each mouse group were used for comparison (Huang et al., 2021; Pai et al., 2021).

In addition, tissues were then double-stained with mouse monoclonal anti-PGP9.5 (1:800, Abcam) and rabbit polyclonal anti-5-HT₇ (1:200, Abcam), followed by secondary goat anti-rabbit or anti-mouse IgG conjugated to Alexa Fluor 488 or 546 (1:1000, Invitrogen) for one hour at room temperature. Tissues were then incubated with a Hoechst dye (1 µg/ml in PBS) (Sigma) for 30 minutes. The images were captured using a Zeiss microscope to verify the localization of PGP9.5 and 5-HT₇ immunostaining.

Western Blotting

Intestinal mucosal proteins were extracted with complete radio-immunoprecipitation assay buffer and subjected to electrophoresis (4-13% polyacrylamide). The resolved proteins were then electrotransferred onto polyvinylidene fluoride or nitrocellulose membranes in a semi-dry blotter. Blots were blocked with 5% (w/v) nonfat dry milk in Tris-buffered saline (TBS) or 5% (w/v) bovine serum albumin in TBS with Tween 20 (TBS-T; 0.1% (v/v) Tween-20 in TBS) for one hour, washed with TBS-T, and incubated with a primary antibody at 4°C overnight. The membrane was washed and incubated with a secondary antibody for one hour. After washing, the membranes were incubated with a chemiluminescent solution and signals were detected. The primary antibodies used included mouse monoclonal anti-NGF (1:100, Santa Cruz) and rabbit polyclonal anti-BDNF (1:250, Santa Cruz). A mouse monoclonal anti-β-actin (1:5000, Sigma) was used as a loading control. The secondary antibodies used were horseradish peroxidase-conjugated goat, mouse, or rabbit anti-rabbit IgG (1:1000, Cell Signaling) (Kuo et al., 2015, 2016).

Polymerase chain reaction (PCR)

Total RNA was extracted from whole colonic tissues and cell samples using Trizol reagent (Invitrogen) according to the manufacturer's instructions. The RNA (2 µg) was reverse transcribed with oligo(dT)₁₅ using RevertAid™ First Strand cDNA Synthesis kit (ThermoFisher, Waltham, MA, USA) in a 20 µL reaction volume. Quantitative PCR (qPCR) was performed using an Applied Biosystems StepOnePlus Real-Time PCR System (Applied Biosystems, Waltham, MA, USA). The reaction mixture consisted of 50 ng of RT product, 10 µL of Power SYBR Green PCR Master Mix, and 125 nM specific primer pairs in a final reaction volume of 20 µL. The qPCR primer pairs for mouse and human cells were designed in this study based on the National Center for Biotechnology Information (NCBI) nucleotide sequence of each gene. The protocol was programmed as follows: 95°C for 10 minutes for 1 cycle; 95°C for 15 seconds,

and 60°C for 1 minute for 40 cycles. Each sample was run in duplicate, and the mean threshold cycle (Ct) was determined from the two runs. Gene expression was calculated from the difference of Ct between the target gene and endogenous housekeeping gene encoding for β-actin (*ACTB*) as ΔCt. Subsequently, the ΔΔCt values were calculated by subtracting the mean ΔCt of the control group from those of the experimental groups, and the relative gene expression is expressed as the fold difference ($2^{-\Delta\Delta C_t}$) (Huang et al., 2019; Huang and Yu, 2020; Yu et al., 2022).

In another setting, semi-quantitative PCR was performed to analyze growth-associated protein 43 (Gap43) expression in the colonic mucosal samples. The cDNA samples were added into a master mix containing 1X PCR buffer, 1 U DreamTaq™ DNA Polymerase, 0.2 mM dNTPs mixture, 0.4 µM forward primer, and 0.4 µM reverse primer. The DNA thermal cycler was programmed to perform a protocol as follows: 95°C for 3 min for 1 cycle; 95°C for 30 sec (denaturation), X°C for 30 sec (annealing, T_m), and 72°C for 30 sec (extension) for 30 cycles; and 72°C for 7 min for final extension. The PCR reaction was performed by using primer pairs for Gap43 (forward: 5'-AGCCAAGGA GGAGCCTAAAC-3' and reverse: 5'-TCAGGCATGT TCTTGGTCAG-3'; T_m=54°C) and β-actin (forward: 5'-GGGAAATCGTGCGTGAC-3' and reverse: 5'-CAAGAAGGAAGGCTGGAA-3'; T_m=55°C) (Dothel et al., 2015). Negative controls were performed with samples that was not reverse transcribed. The PCR products were then electrophoresed in a 1.5% agarose gel in the presence of 0.5 µg/mL ethidium bromide, visualized with an ultraviolet transilluminator, and photographed. The intensity of the DNA bands was analyzed using Gel-Pro Analyzer 4.0 software.

Cell cultures

Human neuroblastoma SH-SY5Y cells were used for the measurement of nerve fiber length and qPCR analysis as described (Dothel et al., 2015; Hsu et al., 2016; Chang et al., 2022). For neurite length studies, cells were plated at 2x10³ cells/ml overnight and treated with 10 µM all-trans retinoic acid (RA) (Sigma) daily for three days to induce differentiation. The cells were pretreated with CYY or SB7 at various concentrations ranging from 0.01 to 100 µM and then incubated with bacteria-free colonic supernatant (see below) in serum-free medium for four days by adding supernatant samples every two days for analysis of neurite outgrowth. The IC₅₀ of compounds to suppress neurite outgrowth was calculated using GraphPad Prism software (GraphPad Software Inc., CA, USA).

In other settings, cells were stimulated with 1 µM serotonin (Sigma) in a reduced serum medium (2% FBS) for 48 hours for measurement of neurite length. For groups of combined treatment with neurotrophins, cells were stimulated with 1 µM serotonin in the presence of 100 ng/ml recombinant NGF (RD Systems) and

Gut hyperalgesia via 5-HT₇ activation

recombinant BDNF (Sigma-Aldrich) in serum-free medium for 48 hours for measurement of neurite length. Alternatively, SH-SY5Y cells were seeded at a density of 1×10^5 cells/ml in 12-well plates overnight and were stimulated with 1 μ M serotonin in the presence of antagonists to 5-HT receptor subtypes for quantitative PCR analysis.

Bacteria-free mouse colonic supernatant

Whole colonic tissues (1 cm) were homogenized in a serum-free medium at a ratio of 1 mg of tissue to 10 μ l medium on ice as described (Hsu et al., 2016; Chang et al., 2022). One tablet of complete-Mini[®] (C-M) (Roche, Mannheim, Germany) was dissolved in 10 ml of serum-free medium for tissue homogenization. The protease inhibitor cocktail was used to prevent the proteolytic activity of gut supernatant, which might cause cell death of SH-SY5Y cultures. Tissue lysate was centrifuged at 10000xg for 10 min at 4°C and the supernatant was collected. The supernatant was mixed with 20-times volume of serum-free medium with C-M and passed through a sterilized filter with 0.45 μ m pore size (Merck Millipore, Darmstadt, Germany). The bacteria-free supernatant was diluted with serum-free medium without C-M at a ratio of 1: 100 and then added to SH-SY5Y cells.

Analysis of neurite outgrowth

The measurement of nerve fiber length was performed following established protocols (Hsu et al., 2016; Chang et al., 2022). Briefly, SH-SY5Y cells were photographed with a microscope equipped with a digital camera. The length of nerve fibers was determined using imaging software (ImageJ 1.47v). The average length of nerve fibers and the percentage of neurons with fibers longer than 50 μ m were calculated from a total of 250-300 neurons per treatment group.

Statistical analysis

All values were expressed as mean \pm SEM. When more than three groups were compared, the one-way analysis of variance was chosen to examine differences between groups, and Tukey's multiple comparison test or Student-Newman-Keuls test was selected as a *post-hoc* test where applicable (GraphPad Prism v. 5.01). An unpaired *t*-test with Welch's test is adopted when the two sample groups are unpaired and normally distributed. Moreover, the IC50 of compounds was compared using Extra-sum-of-squares F-tests. Significance was established at $P < 0.05$.

Results

Analgesic effects of a novel 5-HT₇ antagonist compared to reference standards in IBS-like mouse models

Two models of IBS-like visceral hypersensitivity

were used, including the GW model where mice were subjected to a dual trigger of *Giardia* postinfection combined with water avoidance stress, and the PT model of mice post-resolution of trinitrobenzene sulfonic acid-induced colitis (Feng et al., 2012; Lapointe et al., 2015; Hsu et al., 2016; Chang et al., 2022). Intestinal nociception was evaluated in the two mouse models and their respective control groups by measuring VMR values upon colorectal distension (Fig. 1A,B). We compared the analgesic effects of orally administered CYY, which is a novel and selective 5-HT₇ antagonist, against reference standards used for the treatment of diarrhea-predominant IBS, including ALN (a selective 5-HT₃ antagonist) and LPM (an opioid receptor agonist). Administration of CYY at 5 mg/kg p.o. showed a more potent analgesic effect than ALN and LPM in the two mouse models (Fig. 1C,D).

Intestinal histology was assessed in the mouse models administered vehicle, CYY, ALN, or LPM. Normal colonic morphology was observed in the GW and PT mouse models and their respective control groups, supporting that intestinal hypernociception was not accompanied by any structural abnormality (Fig. 1E,F). Moreover, all mice administered CYY or LPM also showed normal intestinal histopathology (Fig. 1E,F). Of note, colonic hyperemia and granulocyte infiltration were observed in 28% of the GW mice administered ALN (Fig. 1E). A charcoal meal assay was performed to assess the intestinal transit time in the GW and PT mouse models. No difference in intestinal transit time was observed in mice treated with CYY or ALN. A decrease in bowel movement was noted after LPM administration in PT mice (Fig. 1G,H).

Distinct patterns of 5-HT receptor subtypes in mouse intestinal mucosa

Immunofluorescent staining was performed to locate the expression of 5-HT receptor subtypes, including 5-HT₃, 5-HT₄, and 5-HT₇, in the colonic tissues of GW and PT mouse models (Figs. 2, 3). Fiber-like staining of PGP9.5 (a pan-neuronal marker) and punctate patterns of 5-HT₇ were noted in the mucosal regions of colonic tissues of GW mice but not of control mice (Fig. 2A,B). The expression of 5-HT₃ and 5-HT₄ receptors was observed mainly on the epithelia and other cellular structures in the lamina propria of GW mice (Fig. 2C,D). Quantitative results of fluorescent intensity per area showed elevated PGP9.5 staining in the colonic mucosa of GW mice compared with that of control mice (Fig. 2E). Increased mucosal 5-HT₃, 5-HT₄, and 5-HT₇ staining were also observed in colonic tissues of GW mice (Fig. 2E). Moreover, the expression of growth-associated protein 43 (*Gap43*), a marker of neural growth cone, was higher in colonic mucosal samples of GW mice compared with those of control mice by semi-quantitative PCR (Fig. 2F).

For the second model, fiber-like PGP9.5 staining and punctate patterns of 5-HT₇ were found in the colonic

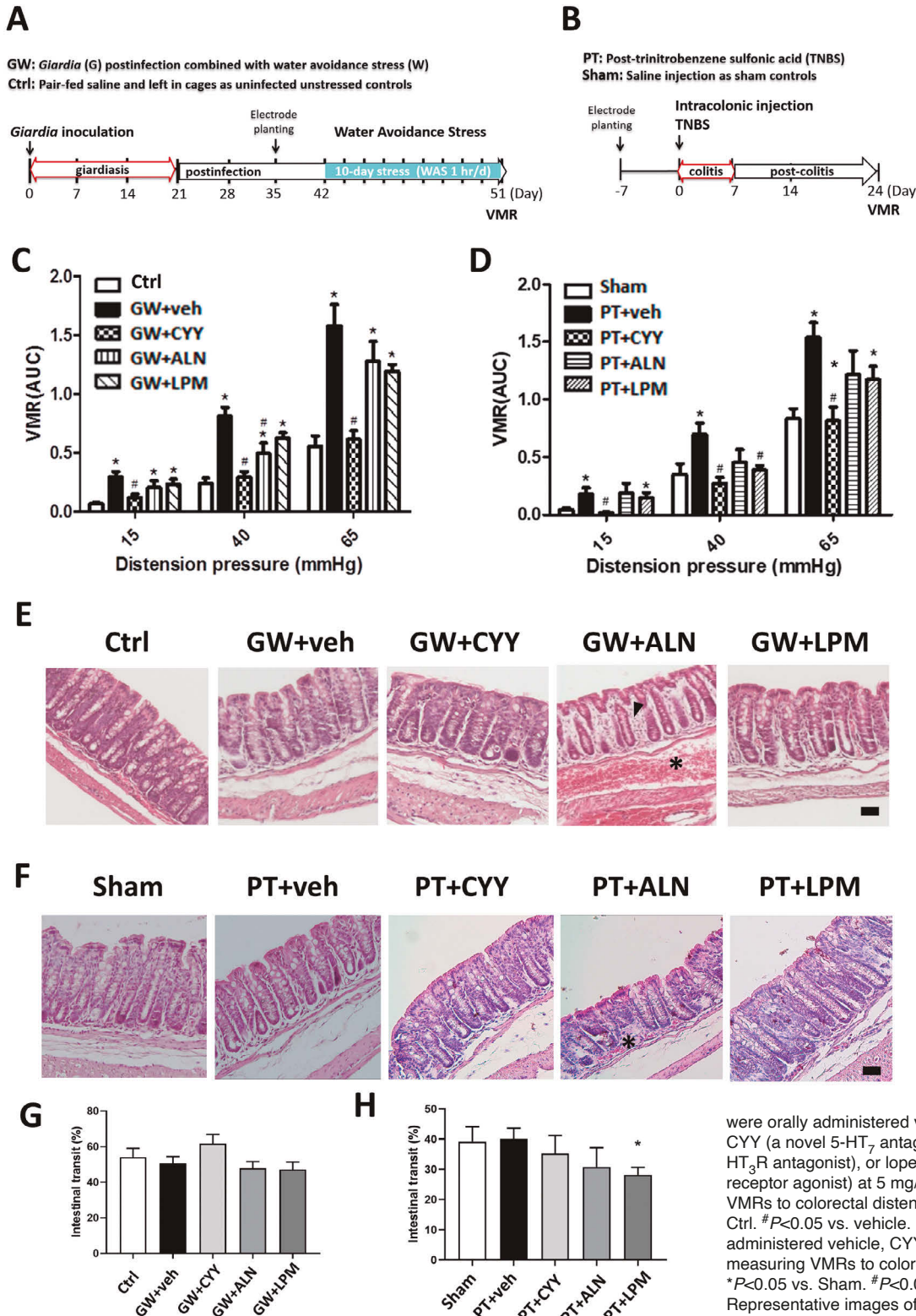


Fig. 1. Comparison of analgesic effects by peroral administration of CYY and reference standards in mice. Two mouse models with IBS-like visceral hypersensitivity were investigated. **A.** Mice were inoculated with *Giardia* trophozoites on day 0 and subjected to water avoidance stress during the post-clearance phase on days 42-51 (designated the GW model). The control (Ctrl) group were uninfected unstressed animals. In previous studies, giardia colonization during the first week and the self-limiting status of parasite infection were confirmed by the absence of trophozoites around 14-21 days. Mice were subjected to water avoidance stress for ten consecutive days during the post-clearance phase to measure visceromotor responses (VMRs) to colorectal distension by electrode planting into abdominal muscles. **B.** Mice were intracolonic injected with trinitrobenzene sulfonic acid (TNBS) on day 0, and those that had recovered from TNBS-induced colitis were assessed for VMRs post-TNBS on day 24 (designated the PT model). The sham-injected (Sham) groups were given the same volume of saline on day 0. Persistent pain in the absence of inflammatory parameters or pathological morphology was previously determined in the colonic tissues of the PT model. **C.** GW mice

were orally administered vehicle or reagents such as CYY (a novel 5-HT₇ antagonist), alosetron (ALN, a 5-HT₃R antagonist), or loperamide (LPM, an opioid receptor agonist) at 5 mg/kg before measurement of VMRs to colorectal distension. N=8/group. *P<0.05 vs. Ctrl. #P<0.05 vs. vehicle. **D.** PT mice were orally administered vehicle, CYY, ALN, or LPM before measuring VMRs to colorectal distension. N=8/group. *P<0.05 vs. Sham. #P<0.05 vs. vehicle. **E.** Representative images of the colonic histology of each treatment group in GW mice. Hyperemia (*) and granulocyte infiltration (arrowheads) were observed in

the ALN but not in the other groups. N=8/group. **F.** Representative images of the colonic histology of each treatment group in PT mice. N=8/group. **G.** **H.** Treatment with CYY and ALN had no effect on bowel movement whereas LPM decreased intestinal transit time in PT mice. N=8/group. *P<0.05 vs. Sham.

Gut hyperalgesia via 5-HT₇ activation

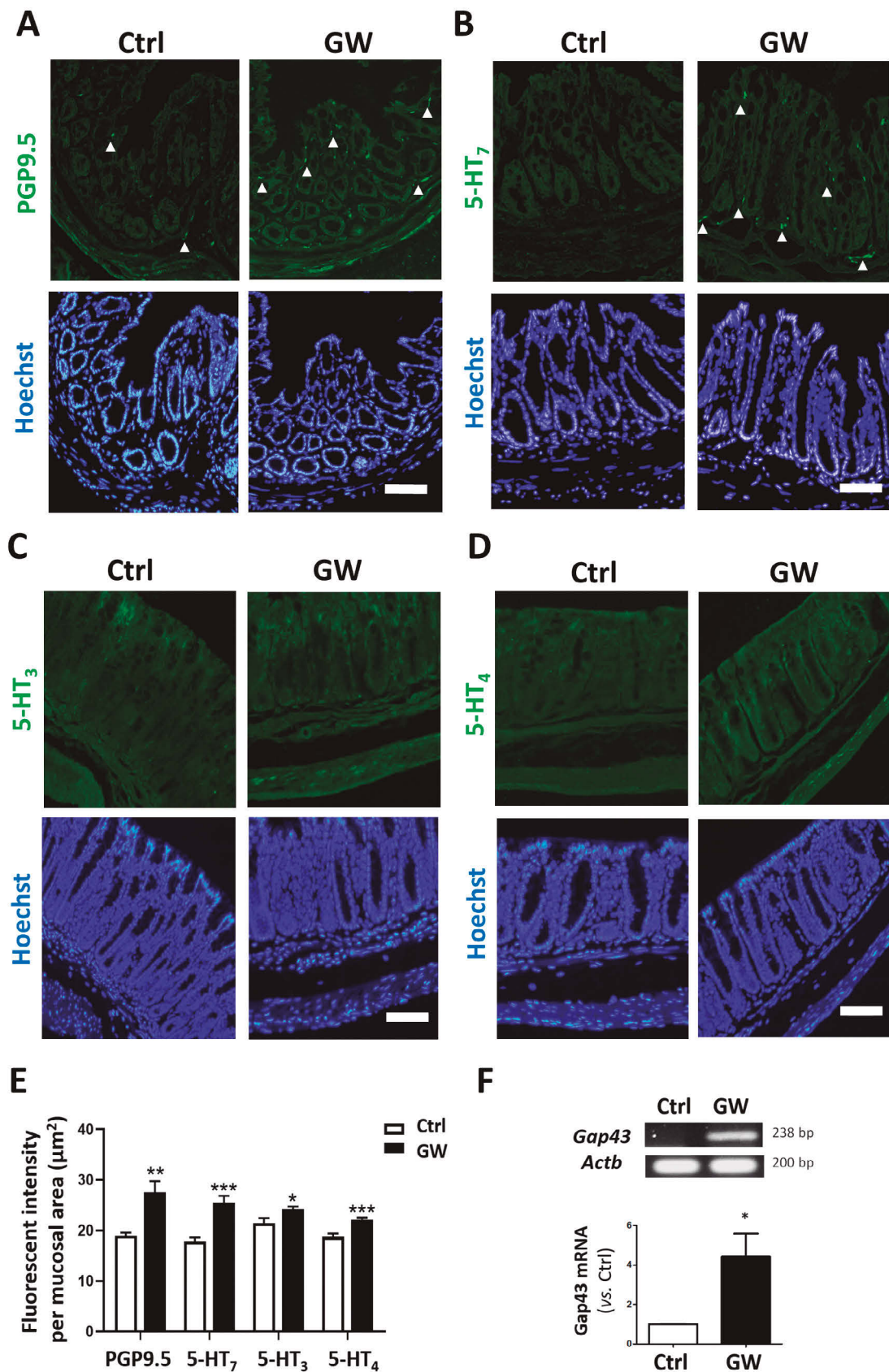


Fig. 2. Fiber-like patterns of PGP9.5 and 5-HT₇ and epithelial staining of 5-HT₃ and 5-HT₄ were observed in the colonic mucosa of GW mice. Representative immunostaining of PGP9.5 (**A**), 5-HT₇ (**B**), 5-HT₃ (**C**), and 5-HT₄ (**D**) in colonic tissues of Ctrl and GW mice. Puncta- or fiber-like patterns were observed for PGP9.5 and 5-HT₇ in mucosal lamina propria, whereas diffuse staining in epithelial layers was noted for 5-HT₃ and 5-HT₄. Cell nuclei were counterstained with a Hoechst dye (blue) to display tissue orientation. **E.** Immunofluorescent intensity per area (µm²) in gut mucosa. A total of 25 images were used for comparison in each group. **P*<0.05, ***P*<0.01, ****P*<0.001 vs. Ctrl. N=5/group. **F.** Levels of growth-associated protein 43 (Gap43, a marker of neural growth cone) in colon tissues of Ctrl and GW mice as determined by semi-quantitative PCR analysis. **P*<0.05 vs. Ctrl. N=5/group.

mucosa of PT mice (Fig. 3A,B). The staining of 5-HT₃ was mainly on epithelial and other cells in the lamina propria of Sham and PT mice (Fig. 3C), and low levels of immunoreactivity were noted for 5-HT₄ in the colonic mucosa of Sham and PT mice (Fig. 3D). Quantitative results showed higher levels of mucosal PGP9.5 staining in PT than in Sham mice (Fig. 3E). Moreover, mucosal 5-HT₇ and 5-HT₃ levels were increased in PT mice; comparable 5-HT₄ levels in the colonic mucosa were noted between PT and sham mice (Fig. 3E). Furthermore, a trend of increased Gap43 expression was also observed in PT mice (Fig. 3F).

Elevated neurotrophins and neurotrophin receptors associated with mucosal neurite outgrowth in mouse colon tissues

As mucosal neurite outgrowth was evident by PGP9.5 immunostaining in the GW and PT mouse models, we further assessed whether 5-HT₇ expression was localized to enteric nerves by double staining. Colocalization of 5-HT₇ expression with PGP9.5-positive nerve fibers was observed in the mucosal region (Fig. 4A). As elevated neurotrophin levels were documented in the biopsy specimens of IBS patients, we next evaluated the levels of neurotrophins and NTRs using qPCR and Western blots in mouse colonic tissues. Higher *Ntrk2* and *Ngfr* gene expression were associated with an increased trend of *Ngf* and *Bdnf* transcripts in GW mice compared with controls (Fig. 4B). Elevated *Bdnf* gene expression and an increased trend of *Ntrk2* transcripts were noted in PT mice (Fig. 4C). A reduction in *Ngfr* gene expression was observed in PT mice (Fig. 4C). Western blotting showed constitutive expression of NGF and BDNF proteins in control mice, suggesting baseline neurotrophin levels in mouse gut tissues (Fig. 4D,E). However, the protein amounts of NGF and BDNF were only slightly higher in GW and PT mice compared with their respective controls, without statistical significance (Fig. 4D,E).

Stimulation with bacteria-free mouse colonic supernatant and exogenous serotonin increased nerve fiber length in a 5-HT₇-dependent manner

A well-established human neuroblastoma cell line, SH-SY5Y, differentiated by retinoic acid was utilized to assess the role of 5-HT₇ in nerve fiber extension. The SH-SY5Y cells incubated with bacteria-free colonic supernatant obtained from GW and PT mice showed longer nerve fiber length than those incubated with colonic supernatant from the respective control groups (Fig. 5A,B). Shorter neurites were observed in those pretreated with CYY *in vitro* at various concentrations (Fig. 5A,B). In addition, neurons stimulated with exogenous 5-HT and LP-211 (a 5-HT₇ agonist) also exhibited longer nerve fibers (Fig. 5C). The average fiber length in each treatment group was quantified from a total of 250-300 neurons and the representative images

were shown (Fig. 5D).

Pretreatment with CYY prevented the elongation of nerve fibers induced by mouse colonic supernatant obtained from GW mice in a dose-dependent manner (Fig. 6A,B). A dose-dependent inhibition of neurite outgrowth by CYY was also found on cells incubated with PT mouse colonic supernatant (Fig. 6E,F). Another selective 5-HT₇ antagonist, SB-269970 (SB7), known to be unstable via oral routes, was tested in the neural cultures *in vitro*. Reduction of neurite length by SB7 was observed in neurons incubated with colonic supernatant from GW (Fig. 6C,D) and PT mice (Fig. 6G,H). The IC₅₀ of compounds to suppress neurite outgrowth was calculated, showing that the IC₅₀ doses of CYY were statistically lower than SB7 to suppress nerve fiber elongation caused by incubation with GW supernatant (Fig. 6I). However, no differences in IC₅₀ doses were seen between CYY and SB7 when using PT supernatant for incubation with neuron cultures (Fig. 6I). The collective data indicated that gut-derived factors from GW and PT mice were able to promote neurite outgrowth via 5-HT₇-dependent pathways.

Differential regulatory roles of 5-HT₃, 5-HT₄, and 5-HT₇ in the expression of neurotrophin receptor subunits

We hypothesized that 5-HT stimulation may alter the expression of NTR subunits (TrkA, TrkB, and p75^{NTR}) and examined which serotonin receptor subtypes were involved in the upregulation of NTRs in neuronal cells. Stimulation with 5-HT elevated *NTRK1*, *NTRK2*, and *NGFR* gene expression in SH-SY5Y cells (Fig. 7A-C). The 5-HT-induced *NTRK1* upregulation was decreased by CYY and SB7 (selective 5-HT₇ antagonists) but not by ALN (a selective 5-HT₃ antagonist), GR125487 (GR, a selective 5HT₄ antagonist), or LPM (an opioid receptor agonist) (Fig. 7A). The 5-HT-induced *NTRK2* upregulation was partially inhibited by CYY, SB7, ALN, GR, and LPM (Fig. 7B). Moreover, the 5-HT-increased p75^{NTR} expression was reduced by CYY and SB7, whereas ALN or GR had no effect (Fig. 7C). The 5-HT-induced p75^{NTR} upregulation was further increased by pretreatment with LPM (Fig. 7C), suggesting that opioid receptors were involved in the augmentation of serotonin effects on p75^{NTR} expression.

Lastly, SH-SY5Y cells were co-treated with 5-HT and neurotrophins to assess the presence of additive effects on neurite outgrowth on SH-SY5Y cells. Cells treated with a single stimulant of 5-HT or NGF exhibited longer nerve fiber lengths (Fig. 7D). The percentage of neurons with fibers longer than 50 μm was higher after co-treatment with 5-HT and NGF compared with the values of single stimulants (Fig. 7E). Moreover, a single stimulant of 5-HT or BDNF induced neurite outgrowth which was comparable to the fiber length after co-treatment with 5-HT and BDNF (Fig. 7F,G). Overall, our data indicated that serotonin/5-HT₇ activation upregulated the expression of all three NTR subunits (i.e., TrkA, TrkB, and p75^{NTR}), while 5-HT₃ and 5-HT₄

Gut hyperalgesia via 5-HT₇ activation

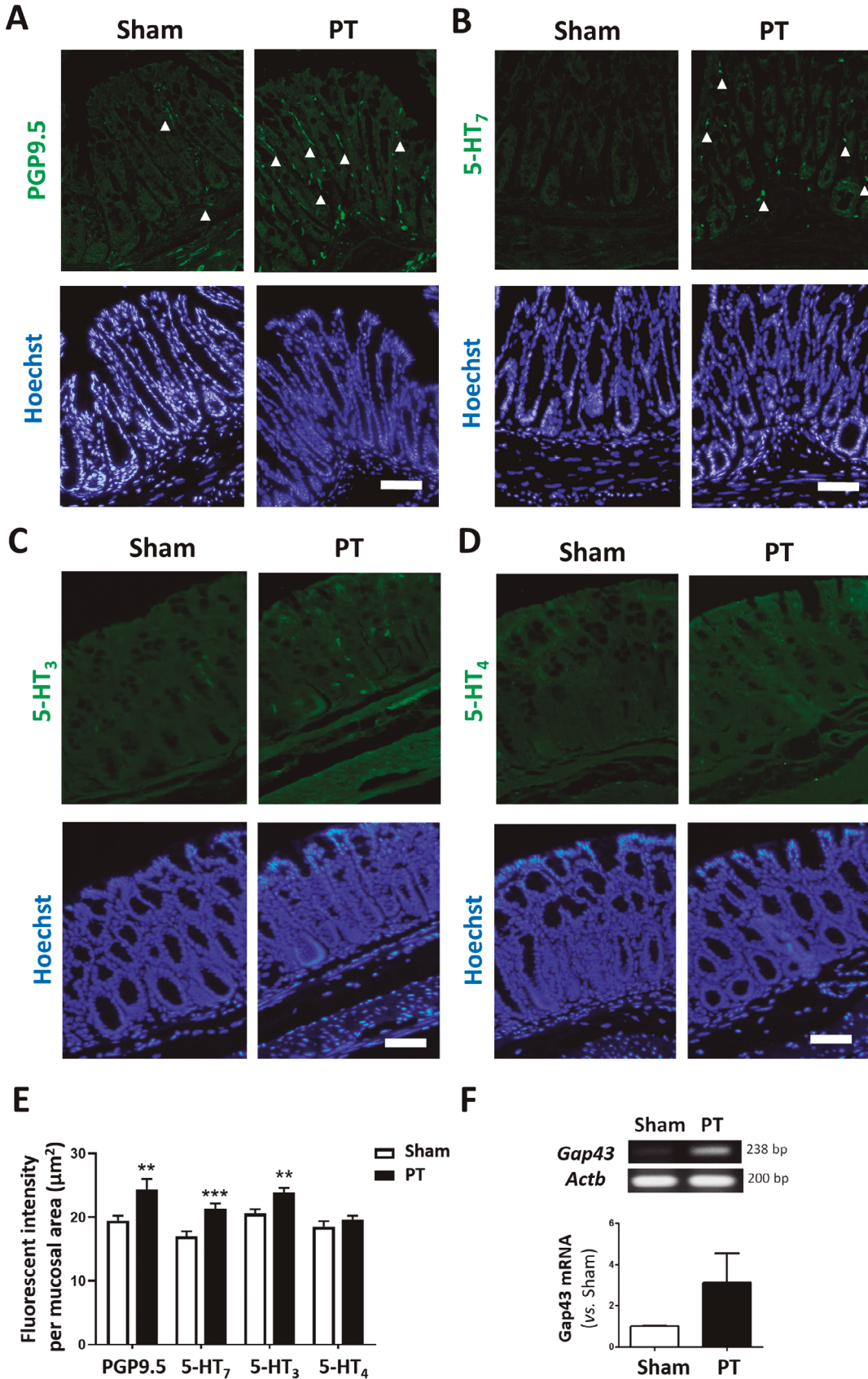


Fig. 3. Fiber-like patterns of PGP9.5 and 5-HT₇ and epithelial staining of 5-HT₃ and 5-HT₄ were observed in the colonic mucosa of PT mice. Representative immunostaining of PGP9.5 (**A**), 5-HT₇ (**B**), 5-HT₃ (**C**), and 5-HT₄ (**D**) in colonic tissues of Sham and PT mice. Puncta- or fiber-like patterns were observed for PGP9.5 and 5-HT₇ in mucosal lamina propria, whereas diffuse staining in epithelial layers and cellular structures was noted for 5-HT₃ and 5-HT₄. Cell nuclei were counterstained with a Hoechst dye (blue) to display tissue orientation. **E.** Immunofluorescent intensity per area (μm²) in gut mucosa. A total of 25 images were used for comparison in each group. ***P*<0.01, ****P*<0.001 vs. Sham. N=5-7/group. **F.** Levels of growth-associated protein 43 (Gap43, a marker of neural growth cone) in colon tissues of Sham and PT mice as determined by semi-quantitative PCR analysis. N=5-7/group. Scale bars: 50 μm.

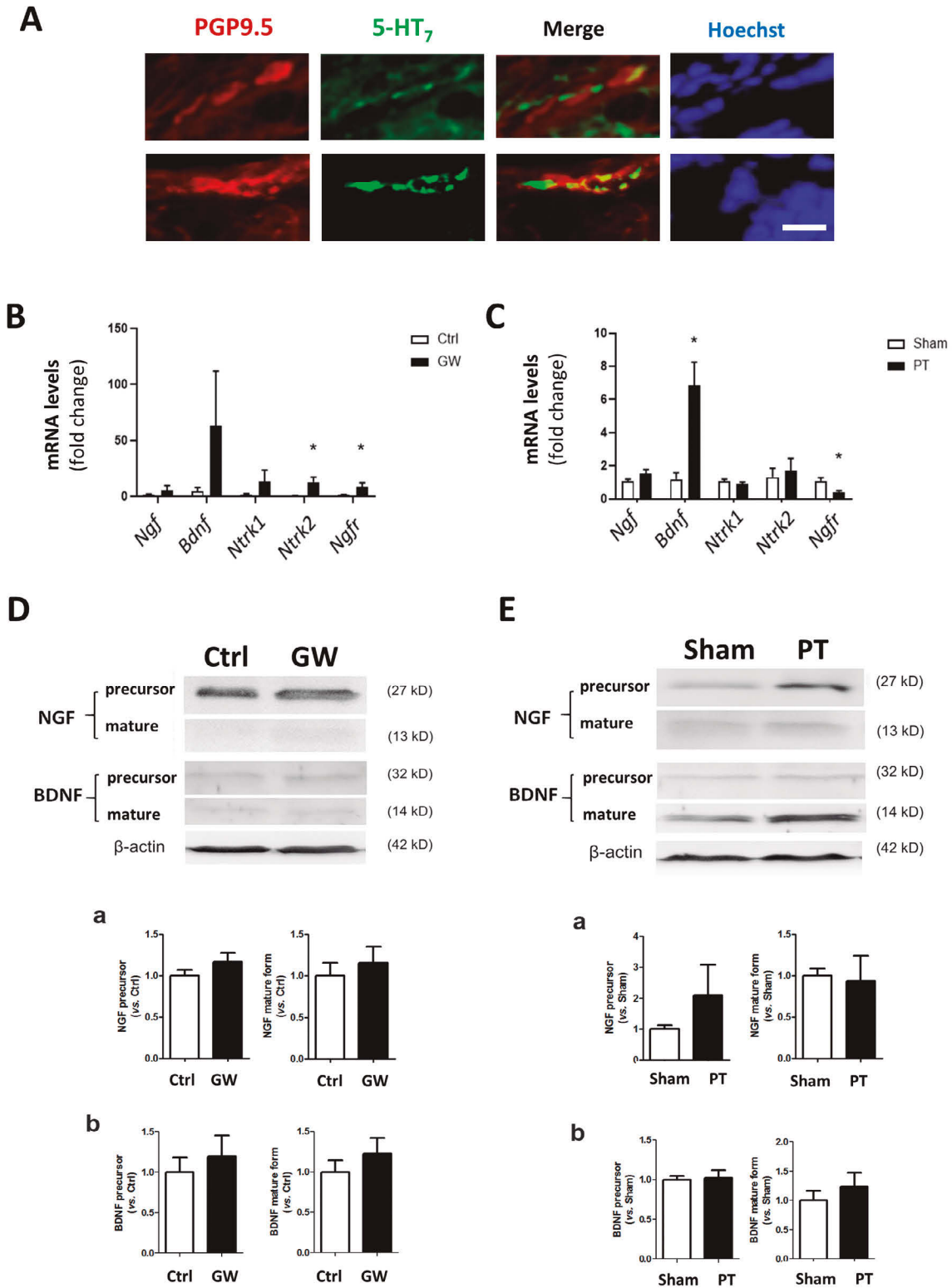
Gut hyperalgesia via 5-HT₇ activation

Fig. 4. Higher neurotrophin and receptor levels correlated with increased mucosal nerve fibers expressing 5-HT₇ in mice. **A.** Representative images showing double staining of PGP9.5 and 5-HT₇ in the colonic mucosa of PT mice. Colocalization of PGP9.5 (red) and 5-HT₇ (green) immunostaining is shown in the merged images. N=5/group. **B, C.** Expression of *Ngf* and *Bdnf* genes and those encoding neurotrophin receptors such as *Ntrk1*, *Ntrk2*, and *Ngfr* in colon tissues of GW and PT mice compared to their respective controls by qPCR analysis. N=5-7/group. **P*<0.05 vs. Ctrl or Sham. **D, E.** Representative Western blots and quantitative results of NGF and BDNF protein levels in colonic mucosal samples of mice. The neurotrophin levels, including precursor and mature forms of NGF, are shown in panel (a) and BDNF in panel (b). N=5/group. Scale bars: 10 μm.

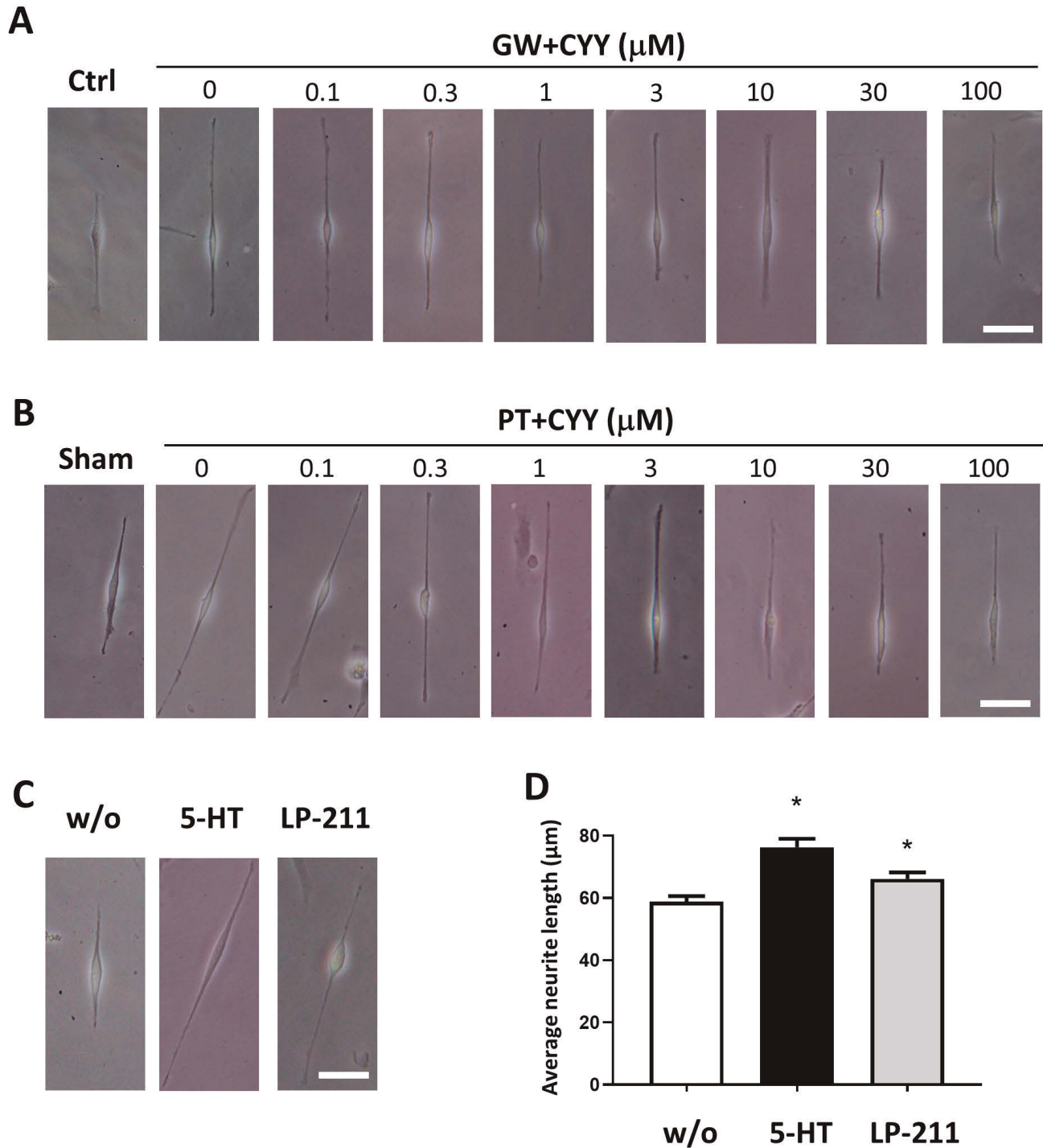


Fig. 5. Representative images of neurons after stimulation with colonic supernatant or exogenous serotonin. Human neuroblastoma SH-SY5Y cells differentiated by retinoic acid (RA) were incubated with bacteria-free mouse intestinal supernatant in the absence or presence of CY7 at various concentrations for assessment of nerve fiber length. **A.** Representative images of neurons following incubation with colonic supernatants of Ctrl and GW mice. **B.** Representative images of neurons following incubation with colonic supernatants of Sham and PT mice. **C.** Representative images of neurons incubated with exogenous 5-HT (1 μM) and a 5-HT₇ agonist LP-211 (1 μM). **D.** Quantitative results of average nerve fiber length in SH-SY5Y cells without treatment (w/o) or after incubation with 5-HT and LP211. A total of 250-300 neurons were used for quantification of nerve fiber length for each group. * $P < 0.05$ vs. w/o. Scale bars: 50 μm .

Gut hyperalgesia via 5-HT₇ activation

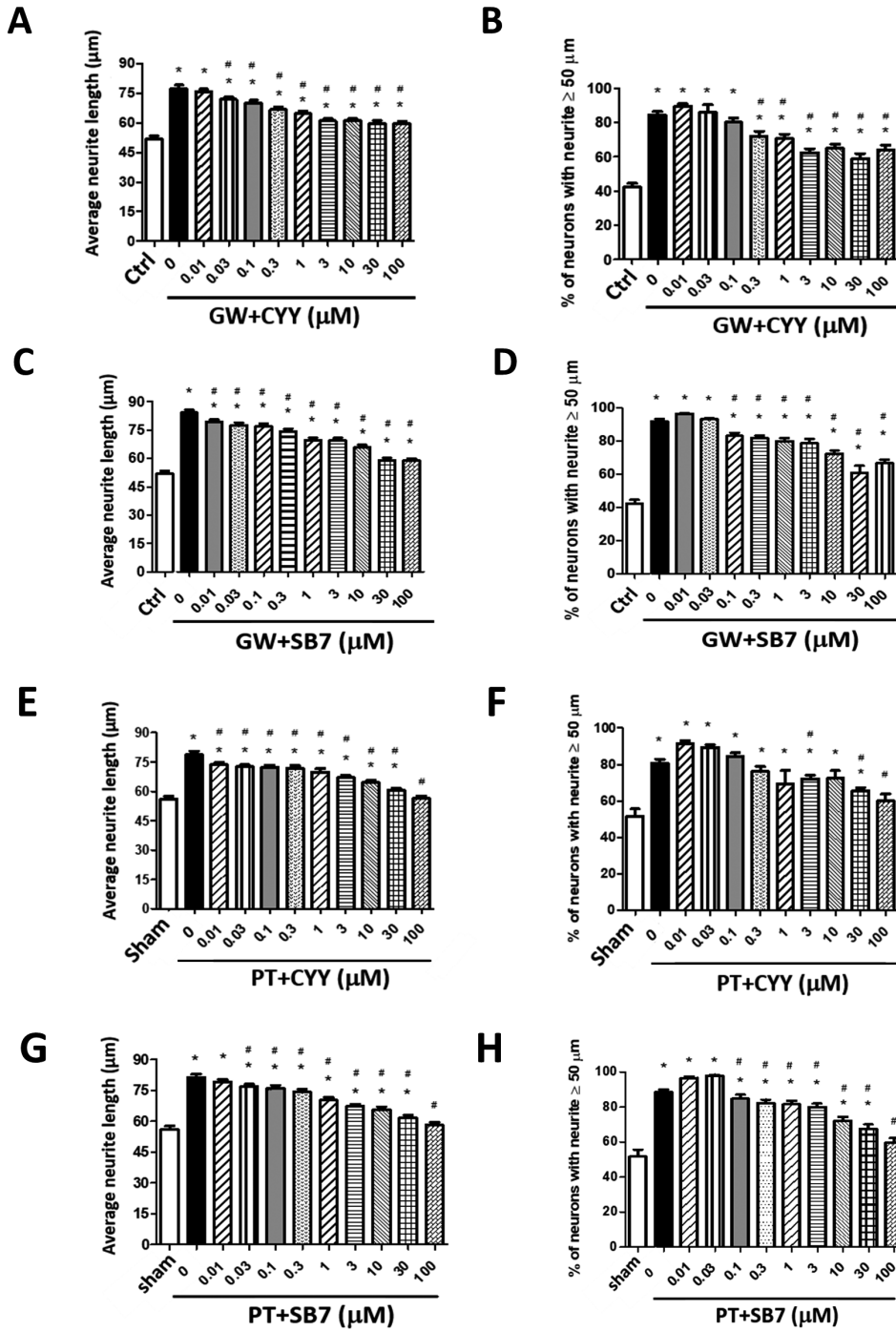


Fig. 6. Stimulation with mouse colonic supernatant induced neurite outgrowth, which CYY dose-dependently inhibited. Human SH-SY5Y cells were incubated with bacteria-free mouse intestinal supernatant in the presence of CYY or SB-269970 (SB7, a selective 5-HT₇ antagonist) at various concentrations ranging from 0.01 to 100 µM for assessment of nerve fiber length. Average neurite length and the percentage of neurons with neurite longer than 50 µm were measured. **A, B.** Neurite length following incubation with colonic supernatants of Ctrl and GW mice in the presence of CYY. **P*<0.05 vs. Ctrl. #*P*<0.05 vs. GW+ 0 µM. **C, D.** Neurite length following incubation with colonic supernatants of Ctrl and GW mice in the presence of SB7. **P*<0.05 vs. Ctrl. #*P*<0.05 vs. GW+ 0 µM. **E, F.** Neurite length after incubation with colonic supernatants of Sham and PT mice in the presence of CYY. **P*<0.05 vs. Sham. #*P*<0.05 vs. PT+ 0 µM. **G, H.** Neurite length after incubation with colonic supernatants of Sham and PT mice in the presence of SB7. **P*<0.05 vs. Sham. #*P*<0.05 vs. PT+ 0 µM. **I.** The IC₅₀ of antagonists to suppress neurite outgrowth stimulated by colonic supernatant or exogenous serotonin. A total of 250-300 neurons were used for quantification of nerve fiber length for each group.

	IC50	CYY (µM)	SB7 (µM)	P-value
Stimulants				
GW colonic supernatant		1.282 ± 0.606	2.919 ± 0.278	0.040
PT colonic supernatant		2.972 ± 0.760	2.130 ± 0.298	0.332

Gut hyperalgesia via 5-HT₇ activation

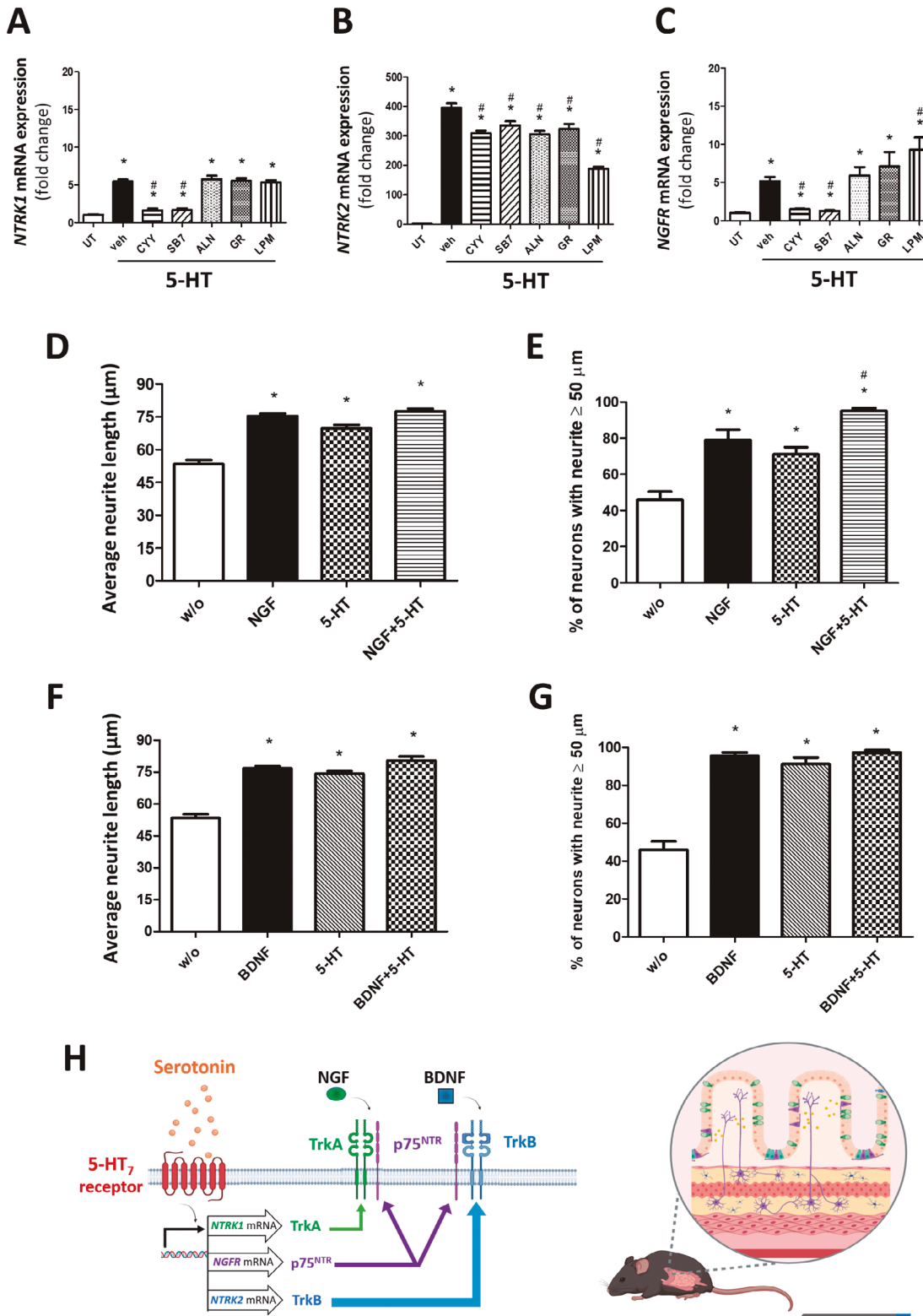


Fig. 7. Serotonin binding to 5-HT₇ upregulated the expression of neurotrophin receptor subunits to promote neurite elongation. SH-SY5Y cells were stimulated with 5-HT and changes in expression levels of neurotrophin receptor (NTR) subunits were analyzed by qPCR. **A-C.** SH-SY5Y cells were either untreated or stimulated with 5-HT (1 μM) in the presence of CYY, SB7, alosetron (ALN, a 5-HT₃ antagonist), GR125487D (GR, a 5-HT₄ antagonist), or loperamide (LPM, an opioid receptor agonist). qPCR results of NTRK1 (**A**), NTRK2 (**B**), and NGFR (**C**) gene expression by 5-HT stimulation. **P*<0.05 vs. untreated (UT); #*P*<0.05 vs. vehicle (veh). *N*=6/group. **D, E.** SH-SY5Y cells were stimulated with recombinant NGF (100 ng/ml) and/or 5-HT (1 μM). Average neurite length and the percentage of neurons with neurites longer than 50 μm after single or co-treatment of NGF and 5-HT. **P*<0.05 vs. w/o; #*P*<0.05 vs. NGF. **F, G.** SH-SY5Y cells were stimulated with recombinant BDNF (100 ng/ml) and/or 5-HT (1 μM). Average neurite length and the percentage of neurons with neurites longer than 50 μm after single or co-treatment of BDNF and 5-HT. **P*<0.05 vs. w/o; #*P*<0.05 vs. BDNF. **H.** Proposed schema of the serotonin/5-HT₇ pathway for upregulation of neurotrophin receptor subunits, including TrkA, TrkB, and p75^{NTR}. The 5-HT₇ pathway played a crucial role in promoting mucosal neurite outgrowth and intestinal hypernociception.

were involved only in TrkB expression. The 5-HT₇ receptor-dependent upregulation of NTR subunits may be involved in mucosal neurite outgrowth and intestinal hyperalgesia (Fig. 7H).

Discussion

IBS represents a substantial clinical problem that accounts for 10-40% of gastroenterology outpatients; however, treatment options for pain management remain limited. Due to the heterogeneous risk factors for IBS development, two experimental models are recommended for nociceptive testing of novel compounds (De Ponti, 2013). Postinfectious and postinflammatory mouse models that showed visceral hypersensitivity upon colorectal distension were assessed in the present study. More potent analgesic effects were observed in the two IBS-like mouse models orally administered a novel 5-HT₇ antagonist, CYY, compared with those given ALN or LPM, reference standards for the clinical management of diarrhea-predominant IBS. We demonstrated that overexpression of 5-HT₇ in mucosal nerve fibers was involved in the pathogenesis of intestinal hypernociception. A new mode of action through upregulation of NTR subunits by 5-HT₇ activation may be involved in neurite outgrowth and intestinal hyperalgesia.

Consistent with the findings of a dense distribution of mucosal nerve fibers in colonic biopsies of IBS patients (Yu et al., 2012; Dothel et al., 2015; Chang et al., 2022), increased levels of PGP9.5 immunostaining, and neural growth cone marker Gap43 were identified in the intestinal mucosa of two IBS-like mouse models. Intestinal neurite outgrowth was also reported in adult rats after neonatal maternal separation, and in hippocampal neurons of preterm pigs with necrotizing enterocolitis (Barreau et al., 2007; Sun et al., 2018), suggesting the presence of aberrant neuroplasticity in various disorders related to gut-brain axis deficits. Ultrastructural changes of the enteric nervous systems were documented in inflammatory bowel diseases and diverticular diseases (Cervi et al., 2017; Alaburda et al., 2020). We showed that serotonin binding to 5-HT₇ promoted the expression of all three NTR subunits (i.e., TrkA, TrkB, and p75^{NTR}), which may potentiate nerve fiber elongation induced by NGF and BDNF. Previous studies using primary hippocampal neurons also demonstrated that 5-HT₇ upregulated TrkB expression and phosphorylation (Samarajeewa et al., 2014). A role of 5-HT₇ in spinogenesis and brain neural development during embryonic and early postnatal stages was previously implicated in anxiety and obsessive-compulsive behaviors (Speranza et al., 2017). In contrast to 5-HT₇, serotonin receptor subtypes 3 and 4 were involved only in the expression of TrkB but not TrkA. The increase in neurotrophins and NTRs in colonic tissues of GW and PT mice was also consistent with the *in vitro* findings. Higher colonic *Ntrk2* and *Ngfr* expression were observed in GW mice, and increased

Bdnf expression was found in PT mice. However, a reduction in *Ngfr* expression encoding for the low-affinity p75^{NTR} protein was also noted in PT mice. Since the p75^{NTR} in complex with high-affinity TrkA and TrkB is responsible for promoting neuronal cell survival and providing neuroprotective effects (Geetha et al., 2012), the downregulation of p75^{NTR} in PT mice is considered a negative feedback mechanism to curb neurite outgrowth for maintaining homeostasis. In sum, the finding implicated a broader effect of 5-HT₇, amongst the family members of serotonin receptors, on the upregulation of a wide range of NTRs for neuroplasticity.

The expression of 5-HT₃, 5-HT₄, and 5-HT₇ was documented in neuron cells *in vitro* (Schill et al., 2020), but recent evidence showed that 5-HT_{2A}, 5-HT₃, and 5-HT₄ immunoreactivity were also found on the colonic epithelia in humans and mice (Ataee et al., 2010; Spohn et al., 2016; Bhattarai et al., 2017, 2018). Herein, immunofluorescent staining showed increased 5-HT₃ and 5-HT₇ receptor protein levels in the colonic mucosa of GW and PT mice compared with their respective control groups, however, with distinct expression patterns. 5-HT₇ staining was observed on mucosal nerve fibers, in contrast to the mainly epithelial localization of 5-HT₃ and 5-HT₄ in our mouse models. The neuron-specific staining of 5-HT₇ in mouse intestines was consistent with the findings in IBS colonic biopsies (Chang et al., 2022). An increase in mucosal 5-HT₄ expression was observed in GW but not PT mice compared with their control groups, suggesting inconsistent mucosal 5-HT₄ levels depending on the triggers to induce visceral hypersensitivity. Locally applying a 5-HT₄ agonist increased neuronal cell numbers in the enteric nervous system associated with more stem-like cells in guinea pig ileum (Matsuyoshi et al., 2010) and increased the maturation of dendritic spines in hippocampal neurons (Schill et al., 2020), supporting its role in neuroplasticity. Nevertheless, accumulating evidence from using organoid cultures and animal models indicated that epithelial 5-HT₃ and 5-HT₄ were involved in serotonin-mediated fluid secretion and crypt proliferation (Gross et al., 2012; Bhattarai et al., 2017, 2018; Park et al., 2019). These findings suggested different modes of action and neuron-specific cell types targeted by 5-HT₇ antagonists compared with those exerted by the 5-HT₃ and 5-HT₄ inhibitors.

As IBS is a disorder with high heterogeneity, these findings bring attention to the need for patient subtype stratification for medical prescription. It is noteworthy that a common anti-diarrheal agent, LPM, had opposite effects on the NTR subunits. The activation of opioid receptors on neurons led to decreased TrkB but increased p75^{NTR} expression. LPM works by inhibiting peristaltic activity through direct effects on smooth muscles of the intestinal wall. Early work showed that LPM inhibited the electrically induced contractions of longitudinal muscle strips isolated from guinea pig ileum through direct binding on the mu-opioid receptors on the

muscles (Mackerer et al., 1976). Later studies indicated that LPM can inhibit the activity of calcium channels such as high-voltage Ca²⁺ channels and large-conductance Ca²⁺-activated K⁺ channels, and diminish the release of acetylcholine triggered by electrical field stimulation (Burleigh, 1988; Vouga et al., 2021). Overall, LPM inhibition on smooth muscle contraction and acetylcholine release contributes to the general anti-diarrheal effects. The *in vitro* data presented herein indicate that aside from its anti-diarrheal indication, LPM may switch neurotrophin sensitivity from BDNF to NGF by upregulating distinct NTR subunit expression. The finding raised caution for the long-term use of LPM in IBS patients with high neurotrophin levels and dense nerve fibers in the intestinal mucosa.

Mouse models of full *Htr7* gene knockout have been established and they did not show aberrant neuronal development in adulthood (Kim et al., 2013). This suggested that despite its neuromodulatory role, serotonin/5-HT₇ was not accountable for essential functions of neuron survival and differentiation as neurotrophins. In contrast, knockout of the *Ngf* or *Bdnf* gene on both alleles caused prenatal death due to the necessity of NGF and BDNF in neural cell survival (Yu et al., 2012; Dothel et al., 2015; Zhang et al., 2019). Heterozygous BDNF(+/-) or NGF(+/-) mice demonstrated decreased VMR values compared with wild-type controls (Yu et al., 2012; Dothel et al., 2015; Zhang et al., 2019). Moreover, TrkA or TrkB knockout mice exhibited the absence of somatosensory afferents and reduced numbers of neurons in the trigeminal ganglion in oral-facial tissues (Matsuo et al., 2001; Ichikawa et al., 2004). Considering the necessity of neurotrophin signaling for neuronal survival, therapeutic intervention with a 5-HT₇ antagonist to alleviate pain symptoms could be more beneficial than targeting neurotrophins for IBS management.

In summary, peroral CYY exhibited stronger analgesic effects compared with reference standards in the two IBS-like mouse models. The 5-HT₇-dependent NTR upregulation and neurite outgrowth may be involved in intestinal hypernociception. An orally active novel 5-HT₇ antagonist could be helpful in the management of IBS-like pain.

Acknowledgements. The authors thank the Animal Centre, Imaging Facility, and Biomedical Resource Core of the First Research Core Laboratory of NTUCM for technical assistance. *Giardia* trophozoites strain GS/M was a kind gift from the laboratory of Dr. Chin-Hung Sun at the Department of Tropical Medicine and Parasitology, National Taiwan University College of Medicine.

Ethics approval. All experimental procedures were approved by the Institute of Animal Care and Use Committee (20160288) of NTUCM.

Competing interests. The authors declare that they have no competing interests.

Availability of data and material. The data and material are available upon request.

Funding. This study was supported by grants from the National Science and Technology Council (NSTC 111-2622-B-002-016), Ministry

of Science and Technology (MOST 110-2622-B-002-013, MOST 110-2320-B-002-011-MY3), National Research Program for Biopharmaceuticals, National Science Council (NSC100-2325-B-002-035, 101-2325-B-002-031, 102-2325-B-002-030), National Health Research Institutes (NHRI-EX111/112/113-11108BI), and National Taiwan University SPARK projects, and Core consortium projects (NTUCC-109L893102, NTUCC-110L891202, NTUCC-111L890602, NTU-CC-112L895002, NTU-CC-113L892702).

Author contribution. Guarantors of the integrity of the entire study: LCY; study concepts and design: LCY and LWH; data acquisition: MPS, YTH, LWL; data analysis/interpretation: MPS, YTH, LWL; statistical analysis: MPS, YTH, LWL; material and technical support: CHT, MSW; obtained funding: MSW, LWH, and LCY; manuscript drafting or revision for important intellectual content, literature research, manuscript editing, and manuscript final version approval: all authors.

References

- Alaburda P., Lukosiene J.I., Pauza A.G., Rysevaite-Kyguoliene K., Kupcinskas J., Saladzinskas Z., Tamelis A. and Pauziene N. (2020). Ultrastructural changes of the human enteric nervous system and interstitial cells of cajal in diverticular disease. *Histol. Histopathol.* 35, 147-157.
- Ataee R., Ajdary S., Rezayat M., Shokrgozar M.A., Shahriari S. and Zarrindast M.R. (2010). Study of 5HT₃ and HT₄ receptor expression in HT29 cell line and human colon adenocarcinoma tissues. *Arch. Iran. Med.* 13, 120-125.
- Atkinson W., Lockhart S., Whorwell P.J., Keevil B. and Houghton L.A. (2006). Altered 5-hydroxytryptamine signaling in patients with constipation- and diarrhea-predominant irritable bowel syndrome. *Gastroenterology* 130, 34-43.
- Barreau F., Cartier C., Leveque M., Ferrier L., Moriez R., Laroute V., Rosztoczy A., Fioramonti J. and Bueno L. (2007). Pathways involved in gut mucosal barrier dysfunction induced in adult rats by maternal deprivation: Corticotrophin-releasing factor and nerve growth factor interplay. *J. Physiol.* 580, 347-356.
- Bhattarai Y., Schmidt B.A., Linden D.R., Larson E.D., Grover M., Beyder A., Farrugia G. and Kashyap P.C. (2017). Human-derived gut microbiota modulates colonic secretion in mice by regulating 5-HT₃ receptor expression via acetate production. *Am. J. Physiol. Gastrointest. Liver Physiol.* 313, G80-G87.
- Bhattarai Y., Williams B.B., Battaglioli E.J., Whitaker W.R., Till L., Grover M., Linden D.R., Akiba Y., Kandimalla K.K., Zachos N.C., Kaunitz J.D., Sonnenburg J.L., Fischbach M.A., Farrugia G. and Kashyap P.C. (2018). Gut microbiota-produced tryptamine activates an epithelial G-protein-coupled receptor to increase colonic secretion. *Cell Host Microbe* 23, 775-785 e775.
- BouSaba J., Sannaa W. and Camilleri M. (2022). Pain in irritable bowel syndrome: Does anything really help? *Neurogastroenterol. Motil.* 34, e14305.
- Burleigh D.E. (1988). Opioid and non-opioid actions of loperamide on cholinergic nerve function in human isolated colon. *Eur. J. Pharmacol.* 152, 39-46.
- Cenac N., Altier C., Motta J.P., d'Aldebert E., Galeano S., Zamponi G.W. and Vergnolle N. (2010). Potentiation of TRPV4 signalling by histamine and serotonin: An important mechanism for visceral hypersensitivity. *Gut* 59, 481-488.
- Cervi A.L., Moynes D.M., Chisholm S.P., Nasser Y., Vanner S.J. and

- Lomax A.E. (2017). A role for interleukin 17A in IBD-related neuroplasticity. *Neurogastroenterol. Motil.* 29, e13112.
- Chang W.Y., Yang Y.T., She M.P., Tu C.H., Lee T.C., Wu M.S., Sun C.H., Hsin L.W. and Yu L.C. (2022). 5-HT₇ receptor-dependent intestinal neurite outgrowth contributes to visceral hypersensitivity in irritable bowel syndrome. *Lab. Invest.* 102, 1023-1037.
- Chen T.L., Chen S., Wu H.W., Lee T.C., Lu Y.Z., Wu L.L., Ni Y.H., Sun C.H., Yu W.H., Buret A.G. and Yu L.C. (2013). Persistent gut barrier damage and commensal bacterial influx following eradication of giardia infection in mice. *Gut Pathog.* 5, 26.
- Corsetti M. and Whorwell P. (2017). New therapeutic options for IBS: the role of the first in class mixed μ -opioid receptor agonist and δ -opioid receptor antagonist (mudelta) eluxadolone. *Expert Rev. Gastroenterol. Hepatol.* 11, 285-292.
- De Ponti F. (2013). Drug development for the irritable bowel syndrome: Current challenges and future perspectives. *Front. Pharmacol.* 4, 7.
- Dickson E.J., Heredia D.J. and Smith T.K. (2010). Critical role of 5-HT_{1A}, 5-HT₃, and 5-HT₇ receptor subtypes in the initiation, generation, and propagation of the murine colonic migrating motor complex. *Am. J. Physiol. Gastrointest. Liver Physiol.* 299, G144-157.
- Dothel G., Barbaro M.R., Boudin H., Vasina V., Cremon C., Gargano L., Bellacosa L., De Giorgio R., Le Berre-Scolin C., Aubert P., Neunlist M., De Ponti F., Stanghellini V. and Barbara G. (2015). Nerve fiber outgrowth is increased in the intestinal mucosa of patients with irritable bowel syndrome. *Gastroenterology* 148, 1002-1011.e4.
- Dunlop S.P., Hebden J., Campbell E., Naesdal J., Olbe L., Perkins A.C. and Spiller R.C. (2006). Abnormal intestinal permeability in subgroups of diarrhea-predominant irritable bowel syndromes. *Am. J. Gastroenterol.* 101, 1288-1294.
- Feng B., La J.H., Tanaka T., Schwartz E.S., McMurray T.P. and Gebhart G.F. (2012). Altered colorectal afferent function associated with TNBS-induced visceral hypersensitivity in mice. *Am. J. Physiol. Gastrointest. Liver Physiol.* 303, G817-824.
- Ford A.C., Sperber A.D., Corsetti M. and Camilleri M. (2020). Irritable bowel syndrome. *Lancet* 396, 1675-1688.
- Ford A.C., Brandt L.J., Young C., Chey W.D., Foxx-Orenstein A.E. and Moayyedi P. (2009). Efficacy of 5-HT₃ antagonists and 5-HT₄ agonists in irritable bowel syndrome: Systematic review and meta-analysis. *Am. J. Gastroenterol.* 104, 1831-1843; quiz 1844.
- Fukudo S., Okumura T., Inamori M., Okuyama Y., Kanazawa M., Kamiya T., Sato K., Shiotani A., Naito Y., Fujikawa Y., Hokari R., Masaoka T., Fujimoto K., Kaneko H., Torii A., Matsueda K., Miwa H., Enomoto N., Shimosegawa T. and Koike K. (2021). Evidence-based clinical practice guidelines for irritable bowel syndrome 2020. *J. Gastroenterol.* 56, 193-217.
- Gao J., Xiong T., Grabauskas G. and Owyang C. (2022). Mucosal serotonin reuptake transporter expression in irritable bowel syndrome is modulated by gut microbiota via mast cell-prostaglandin E₂. *Gastroenterology* 162, 1962-1974.e6.
- Geetha T., Zheng C., Unroe B., Sycheva M., Kluess H. and Babu J.R. (2012). Polyubiquitination of the neurotrophin receptor p75 directs neuronal cell survival. *Biochem. Biophys. Res. Commun.* 421, 286-290.
- Gross E.R., Gershon M.D., Margolis K.G., Gertsberg Z.V., Li Z. and Cowles R.A. (2012). Neuronal serotonin regulates growth of the intestinal mucosa in mice. *Gastroenterology* 143, 408-417.e2.
- Halliez M.C., Motta J.P., Feener T.D., Guerin G., LeGoff L., Francois A., Colasse E., Favennec L., Gargala G., Lapointe T.K., Altier C. and Buret A.G. (2016). Giardia duodenalis induces paracellular bacterial translocation and causes postinfectious visceral hypersensitivity. *Am. J. Physiol. Gastrointest. Liver Physiol.* 310, G574-585.
- Hong S., Zheng G., Wu X., Snider N.T., Owyang C. and Wiley J.W. (2011). Corticosterone mediates reciprocal changes in CB 1 and TRPV1 receptors in primary sensory neurons in the chronically stressed rat. *Gastroenterology* 140, 627-637.e4.
- Hsu L.T., Hung K.Y., Wu H.W., Liu W.W., She M.P., Lee T.C., Sun C.H., Yu W.H., Buret A.G. and Yu L.C. (2016). Gut-derived cholecystokinin contributes to visceral hypersensitivity via nerve growth factor-dependent neurite outgrowth. *J. Gastroenterol. Hepatol.* 31, 1594-1603.
- Huang C.Y. and Yu L.C. (2020). Distinct patterns of interleukin-12/23 and tumor necrosis factor alpha synthesis by activated macrophages are modulated by glucose and colon cancer metabolites. *Chin. J. Physiol.* 63, 7-14.
- Huang C.Y., Huang C.Y., Pai Y.C., Lin B.R., Lee T.C., Liang P.H. and Yu L.C. (2019). Glucose metabolites exert opposing roles in tumor chemoresistance. *Front. Oncol.* 9, 1282.
- Huang Y.J., Lee T.C., Pai Y.C., Lin B.R., Turner J.R. and Yu L.C. (2021). A novel tumor suppressor role of myosin light chain kinase splice variants through downregulation of the TEAD4/CD44 axis. *Carcinogenesis* 42, 961-974.
- Ichikawa H., Matsuo S., Silos-Santiago I., Jacquin M.F. and Sugimoto T. (2004). The development of myelinated nociceptors is dependent upon trks in the trigeminal ganglion. *Acta Histochem.* 106, 337-343.
- Khan N. and Smith M.T. (2015). Neurotrophins and neuropathic pain: Role in pathobiology. *Molecules* 20, 10657-10688.
- Kim J.J. and Khan W.I. (2014). 5-HT₇ receptor signaling: Improved therapeutic strategy in gut disorders. *Front. Behav. Neurosci.* 8, 396.
- Kim J.J., Bridle B.W., Ghia J.E., Wang H., Syed S.N., Manocha M.M., Rengasamy P., Shajib M.S., Wan Y., Hedlund P.B. and Khan W.I. (2013). Targeted inhibition of serotonin type 7 (5-HT₇) receptor function modulates immune responses and reduces the severity of intestinal inflammation. *J. Immunol.* 190, 4795-4804.
- Kobe F., Guseva D., Jensen T.P., Wirth A., Renner U., Hess D., Muller M., Medrihan L., Zhang W., Zhang M., Braun K., Westerholz S., Herzog A., Radyushkin K., El-Kordi A., Ehrenreich H., Richter D.W., Rusakov D.A. and Ponimaskin E. (2012). 5-HT₇R/G12 signaling regulates neuronal morphology and function in an age-dependent manner. *J. Neurosci.* 32, 2915-2930.
- Kuo W.T., Lee T.C., Yang H.Y., Chen C.Y., Au Y.C., Lu Y.Z., Wu L.L., Wei S.C., Ni Y.H., Lin B.R., Chen Y., Tsai Y.H., Kung J.T., Sheu F., Lin L.W. and Yu L.C. (2015). LPS receptor subunits have antagonistic roles in epithelial apoptosis and colonic carcinogenesis. *Cell Death Differ.* 22, 1590-1604.
- Kuo W.T., Lee T.C. and Yu L.C. (2016). Eritoran suppresses colon cancer by altering a functional balance in toll-like receptors that bind lipopolysaccharide. *Cancer Res.* 76, 4684-4695.
- Lambarth A., Zarate-Lopez N. and Fayaz A. (2022). Oral and parenteral anti-neuropathic agents for the management of pain and discomfort in irritable bowel syndrome: A systematic review and meta-analysis. *Neurogastroenterol. Motil.* 34, e14289.
- Lapointe T.K., Basso L., Iftinca M.C., Flynn R., Chapman K., Dietrich G., Vergnolle N. and Altier C. (2015). TRPV1 sensitization mediates postinflammatory visceral pain following acute colitis. *Am. J. Physiol. Gastrointest. Liver Physiol.* 309, G87-99.
- Lee J., Avramets D., Jeon B. and Choo H. (2021). Modulation of serotonin receptors in neurodevelopmental disorders: Focus on 5-HT₇ receptor. *Molecules* 26, 3348.

Gut hyperalgesia via 5-HT₇ activation

- Liu M., Geddis M.S., Wen Y., Setlik W. and Gershon M.D. (2005). Expression and function of 5-HT₄ receptors in the mouse enteric nervous system. *Am. J. Physiol. Gastrointest. Liver Physiol.* 289, G1148-1163.
- Mackerer C.R., Clay G.A. and Dajani E.Z. (1976). Loperamide binding to opiate receptor sites of brain and myenteric plexus. *J. Pharmacol. Exp. Ther.* 199, 131-140.
- Matsumoto K., Lo M.W., Hosoya T., Tashima K., Takayama H., Murayama T. and Horie S. (2012). Experimental colitis alters expression of 5-HT receptors and transient receptor potential vanilloid 1 leading to visceral hypersensitivity in mice. *Lab. Invest.* 92, 769-782.
- Matsuo S., Ichikawa H., Henderson T.A., Silos-Santiago I., Barbacid M., Arends J.J. and Jacquin M.F. (2001). TrkA modulation of developing somatosensory neurons in oro-facial tissues: Tooth pulp fibers are absent in trkA knockout mice. *Neuroscience* 105, 747-760.
- Matsuyoshi H., Kuniyasu H., Okumura M., Misawa H., Katsui R., Zhang G.X., Obata K. and Takaki M. (2010). A 5-HT₄-receptor activation-induced neural plasticity enhances *in vivo* reconstructs of enteric nerve circuit insult. *Neurogastroenterol. Motil.* 22, 806-813.e226.
- Meuser T., Pietruck C., Gabriel A., Xie G.X., Lim K.J. and Pierce Palmer P. (2002). 5-HT₇ receptors are involved in mediating 5-HT-induced activation of rat primary afferent neurons. *Life Sci.* 71, 2279-2289.
- Michel K., Zeller F., Langer R., Nekarda H., Kruger D., Dover T.J., Brady C.A., Barnes N.M. and Schemann M. (2005). Serotonin excites neurons in the human submucosal plexus via 5-HT₃ receptors. *Gastroenterology* 128, 1317-1326.
- Monro R.L., Bornstein J.C. and Bertrand P.P. (2005). Slow excitatory post-synaptic potentials in myenteric AH neurons of the guinea-pig ileum are reduced by the 5-hydroxytryptamine₇ receptor antagonist SB269970. *Neuroscience* 134, 975-986.
- Nee J., Zakari M. and Lembo A.J. (2015). Current and emerging drug options in the treatment of diarrhea predominant irritable bowel syndrome. *Expert Opin. Pharmacother.* 16, 2781-2792.
- Pai Y.C., Weng L.T., Wei S.C., Wu L.L., Shih D.Q., Targan S.R., Turner J.R. and Yu L.C. (2021). Gut microbial transcytosis induced by tumor necrosis factor-like 1A-dependent activation of a myosin light chain kinase splice variant contributes to IBD. *J. Crohns Colitis* 15, 258-272.
- Pai Y.C., Li Y.H., Turner J.R. and Yu L.C. (2023). Transepithelial barrier dysfunction drives microbiota dysbiosis to initiate epithelial clock-driven inflammation. *J. Crohns Colitis* 17, 1471-1488.
- Park C.J., Armenia S.J., Zhang L. and Cowles R.A. (2019). The 5-HT₄ receptor agonist prucalopride stimulates mucosal growth and enhances carbohydrate absorption in the ileum of the mouse. *J. Gastrointest. Surg.* 23, 1198-1205.
- Ren T.H., Wu J., Yew D., Ziea E., Lao L., Leung W.K., Berman B., Hu P.J. and Sung J.J.Y. (2007). Effects of neonatal maternal separation on neurochemical and sensory response to colonic distension in a rat model of irritable bowel syndrome. *Am. J. Physiol. Gastrointestinal. Liver Physiol.* 292, G849-G856.
- Samarajeewa A., Goldemann L., Vasefi M.S., Ahmed N., Gondora N., Khanderia C., Mielke J.G. and Beazely M.A. (2014). 5-HT₇ receptor activation promotes an increase in TrkB receptor expression and phosphorylation. *Front. Behav. Neurosci.* 8, 391.
- Schill Y., Bijata M., Kopach O., Cherkas V., Abdel-Galil D., Bohm K., Schwab M.H., Matsuda M., Compan V., Basu S., Bijata K., Wlodarczyk J., Bard L., Cole N., Dityatev A., Zeug A., Rusakov D.A. and Ponimaskin E. (2020). Serotonin 5-HT₄ receptor boosts functional maturation of dendritic spines via RhoA-dependent control of F-actin. *Commun. Biol.* 3, 76.
- Speranza L., Labus J., Volpicelli F., Guseva D., Lacivita E., Leopoldo M., Bellenchi G.C., di Porzio U., Bijata M., Perrone-Capano C. and Ponimaskin E. (2017). Serotonin 5-HT₇ receptor increases the density of dendritic spines and facilitates synaptogenesis in forebrain neurons. *J. Neurochem.* 141, 647-661.
- Spohn S.N., Bianco F., Scott R.B., Keenan C.M., Linton A.A., O'Neill C.H., Bonora E., Dickey M., Lavoie B., Wilcox R.L., MacNaughton W.K., De Giorgio R., Sharkey K.A. and Mawe G.M. (2016). Protective actions of epithelial 5-hydroxytryptamine 4 receptors in normal and inflamed colon. *Gastroenterology* 151, 933-944.e3.
- Sun J., Pan X., Christiansen L.I., Yuan X.L., Skovgaard K., Chatterton D.E.W., Kaalund S.S., Gao F., Sangild P.T. and Pankratova S. (2018). Necrotizing enterocolitis is associated with acute brain responses in preterm pigs. *J. Neuroinflamm.* 15, 180.
- Tonini M., Vicini R., Cervio E., De Ponti F., De Giorgio R., Barbara G., Stanghellini V., Dellabianca A. and Sternini C. (2005). 5-HT₇ receptors modulate peristalsis and accommodation in the guinea pig ileum. *Gastroenterology* 129, 1557-1566.
- Vouga A.G., Rockman M.E., Yan J., Jacobson M.A. and Rothberg B.S. (2021). State-dependent inhibition of BK channels by the opioid agonist loperamide. *J. Gen. Physiol.* 153.
- Yaakob N.S., Chinkwo K.A., Chetty N., Coupar I.M. and Irving H.R. (2015). Distribution of 5-HT₃, 5-HT₄, and 5-HT₇ receptors along the human colon. *J. Neurogastroenterol. Motil.* 21, 361-369.
- Yu Y.B., Zuo X.L., Zhao Q.J., Chen F.X., Yang J., Dong Y.Y., Wang P. and Li Y.Q. (2012). Brain-derived neurotrophic factor contributes to abdominal pain in irritable bowel syndrome. *Gut* 61, 685-694.
- Yu F.Y., Huang S.G., Zhang H.Y., Ye H., Chi H.G., Zou Y., Lv R.X. and Zheng X.B. (2016). Comparison of 5-hydroxytryptophan signaling pathway characteristics in diarrhea-predominant irritable bowel syndrome and ulcerative colitis. *World J. Gastroenterol.* 22, 3451-3459.
- Yu L.C., Wei S.C., Li Y.H., Lin P.Y., Chang X.Y., Weng J.P., Shue Y.W., Lai L.C., Wang J.T., Jeng Y.M. and Ni Y.H. (2022). Invasive pathobionts contribute to colon cancer initiation by counterbalancing epithelial antimicrobial responses. *Cell. Mol. Gastroenterol. Hepatol.* 13, 57-79.
- Zhang L.Y., Dong X., Liu Z.L., Mo J.Z., Fang J.Y., Xiao S.D., Li Y. and Chen S.L. (2011). Luminal serotonin time-dependently modulates vagal afferent driven antinociception in response to colorectal distention in rats. *Neurogastroenterol. Motil.* 23, 62-69.e66.
- Zhang Y., Qin G., Liu D.R., Wang Y. and Yao S.K. (2019). Increased expression of brain-derived neurotrophic factor is correlated with visceral hypersensitivity in patients with diarrhea-predominant irritable bowel syndrome. *World J. Gastroenterol.* 25, 269-281.
- Zou B.C., Dong L., Wang Y., Wang S.H. and Cao M.B. (2007). Expression and role of 5-HT₇ receptor in brain and intestine in rats with irritable bowel syndrome. *Chin. Med. J.* 120, 2069-2074.